Mechanistic Elucidation of the Arylation of Non-Spectator *N*-Heterocyclic Carbenes at Copper using a Combined Experimental and Computational Approach.

Thomas J. Williams,[a] Joshua T. W. Bray,[a] Benjamin R. M. Lake,[b] Charlotte E. Willans,[b]* Nasir A. Rajabi,[c] Alireza Ariafard,[c,d]* Chiara Manzini,[a,e] Fabio Bellina,[e] Adrian C. Whitwood,[a] and Ian J. S. Fairlamb[a]*

[a] Department of Chemistry, University of York, Heslington, York YO10 5DD, UK.

[b] School of Chemistry, University of Leeds, Woodhouse Lane, Leeds, LS2 9JT, UK.

[c] Department of Chemistry, Faculty of Science, Central Tehran Branch, Islamic Azad University, Shahrak Gharb, Tehran, Iran.

[d] School of Chemistry, University of Tasmania, Private Bag 75, Hobart TAS 7001, Australia.

[e] Dipartimento di Chimica e Chimica Industriale, University of Pisa, via Risorgimento 35, 56126 Pisa, Italy.

Supporting Information is available for this paper.

ABSTRACT: Cu^{I}(NHC)Br complexes (NHC = *N*-heterocyclic carbene) undergo a direct reaction with iodobenzene to give 2-arylated benzimidazolium products. The nature of the *N*-substituent on the NHC ligand influences the reactivity of the Cu^{I}(NHC)Br complex towards arylation. *N*-Benzyl or *N*-phenyl substituents facilitate arylation, whereas *N*-mesityl substituents hinder arylation. Density functional theory calculations show that an oxidative addition/reductive elimination pathway, involving Cu^{III} species, is energetically feasible. A less hindered Cu^{I}(NHC)Br complex, with *N*-benzyl groups, is susceptible to oxidation reactions to give 1,3-dibenzylbenzimidazolium cations containing a $Cu^{I}Br_x$ anion (various polymorphs). The results described herein are of relevance to C-H functionalization of benz(azoles).

Introduction

The C-H bond functionalization of heteroarenes to form biaryl species has attracted considerable attention in recent years, becoming an increasingly viable alternative to traditional cross-coupling reactions with organometallic reagents.[1,2] The resulting materials are important substructures in a range of pharmaceutical and agrochemical products. The development of dual Pd/Cu-mediated approaches for the functionalization of (benz)azoles, and related purines, has greatly diversified the arylated derivatives that can be accessed.[3-5] For these processes it can be beneficial to use stoichiometric quantities of a Cu salt with Pd acting as a catalyst; however, the reaction mechanism is not fully understood.

From a synthetic methodology perspective, Bellina and co-workers have developed the functionalization of imidazoles to yield 2-arylimidazoles, which proceed in DMF at high temperatures (Scheme 1a).[6-12] Adenosine can be functionalized using a similar route, to give 8-aryladenosine (Scheme 1b).[13,14] The functionalization of a benzimidazole to give a 2-arylbenzimidazole has been shown to proceed in the absence of Pd and using stoichiometric quantities of CuI, though higher reaction temperatures were employed in this reaction (Scheme 1c).[15] Interestingly, Miura and co-workers commented in their work that the arylation of 1-methylbenzimidazole works considerably better with CuI alone than using Pd/Cu together – the reasons for this outcome was stated as unclear at the time.[15b] Mechanisms for the Pd/Cu-mediated reactions have been proposed, with suggestions of initial intermediates involving *N*-coordination of Cu^{I} to imidazole, organocupurate formation and involvement of Cu^{I}-NHCs.[6-14]

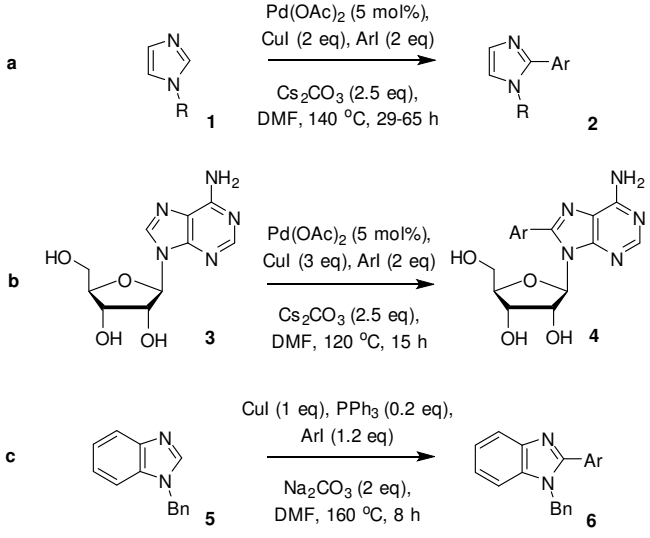

Scheme 1. Leading examples of C-H bond functionalization reactions at heteroarenes.

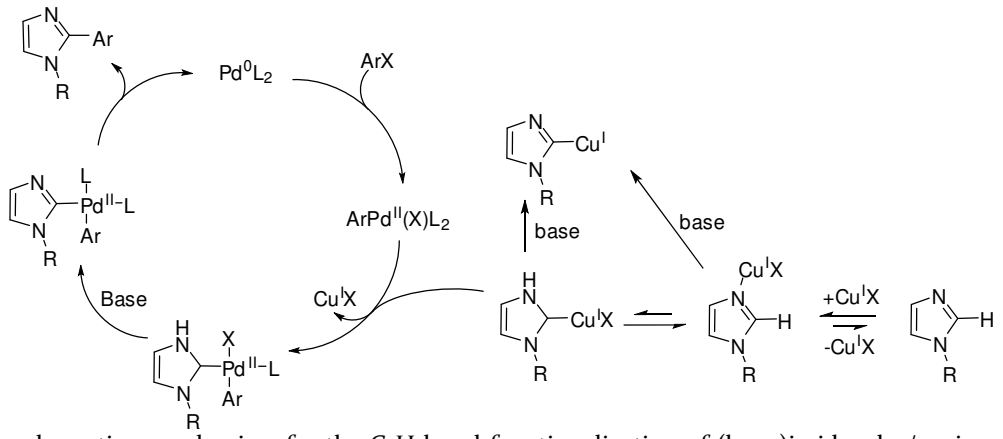

Scheme 2. Proposed reaction mechanism for the C-H bond functionalization of (benz)imidazoles/purines, mediated by Pd and Cu. The Pd^0L_2 is likely in equilibrium with higher order Pd nanoparticles (not shown). Note: delocalization of electron density on to the carbenic carbon atom is not shown in these structures, neither in subsequent structures in the paper.

Metal-NHCs have also been postulated in intramolecular Rh-catalyzed C-H functionalization of benzimidazoles,[16] and in intermolecular Rh-catalyzed C-H functionalization of heterocycles.[17] A pathway bringing the proposed Pd/Cu-mediated mechanisms together is shown in Scheme 2, which provides a route to transferring an NHC ligand from Cu^I to Pd^{II}, allowing reductive elimination to form the arylated imidazole. It has also been established that well-defined Pd nanoparticles are formed under these reaction conditions, with their role most likely as a reservoir of Pd^0,[18] akin to Heck-type coupling reactions.[19,20] At this point it is important to state that the role of Pd can be viewed as increasing the reactivity of the aryl electrophile, where $[Pd(I)(Ph)(L)_2]$ would be much more reactive toward a Cu-NHC species than PhI alone.

Under working conditions the proposed intermediate species in Scheme 2 are difficult to detect, and indeed, synthesize, especially at Cu^I. Very recent studies by Hahn *et al.* showed that organoplatinate caffeine-derived species can be formed by an alternative synthetic route involving oxidative addition of Pt^0 into a C-Br bond.[21] Subsequent protonation gave a Pt^{II}- NHC complex of the type $Pt^{II}(X)_2(NHC)L$. While this study confirms the potential of M-NHC species as intermediates, the reactivity of these complexes toward aryl halides, for example, has not been studied.

To address the issue of whether Cu^I-NHC species can be arylated by reaction with aryl iodide (in the presence and absence of Pd), a series of model compounds (**7**-**9**) were identified (Figure 1a). The *N*-benzyl in **7** provides modest steric protection at the carbene center, and is similar to typical substrates (*e.g.* **5** in Scheme 1). The second benzyl substituent, however, takes the place of a proton. The effect of steric bulk around the carbene center was investigated by exchanging the benzyl substituents for phenyl (compound **8**), in addition to removing the benzo-backbone (compound **9**) to examine if C4-H/C5-H bond activation can also occur.

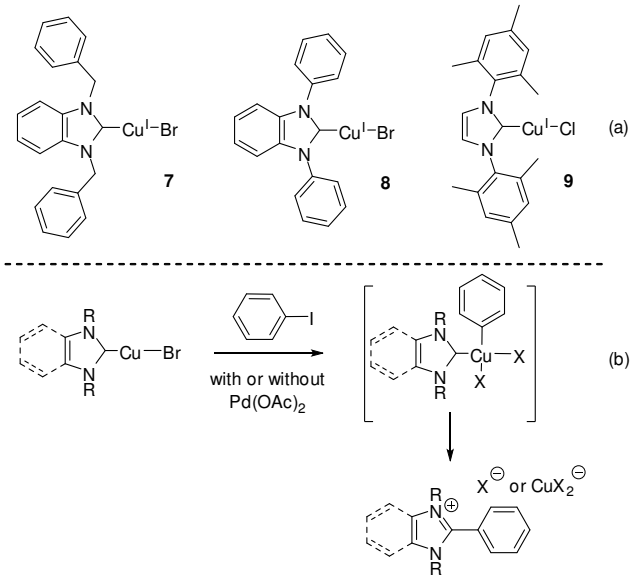

Figure 1. (a) Cu^I-NHC complexes examined in C2 functionalization. (b) reaction of Cu^I-NHC complexes with PhI in the presence and absence of $Pd(OAc)_2$, *via* a Cu^{III} species.

A key question arising from this study is whether the NHC ligand acts in either a non-interfering and supporting manner (*i.e.* as a spectator ligand) or participates (*e.g.* as an actor and hence substrate)? Whilst metal-NHC complexes are generally robust species, reductive elimination can occur from Ni^{II} and Pd^{II} complexes containing NHC and aryl or alkyl ligands.[22-26] Therefore, this study would allow us to understand whether reductive elimination is feasible at Cu *via* a putative higher oxidation state intermediate (a potential pathway is highlighted in Figure 1b).

Results and Discussion

Synthesis of Cu^{I}-NHC complexes 7-9. Our studies on the synthesis of **7** started with the reaction of 1,3-dibenzylbenzimidazolium bromide **10** with Cu_2O in water at reflux.[27] First attempts at this reaction were hindered by oxidation reactions where a Cu^{I} salt, containing the 1,3-dibenzylbenzimidazolium cation, was formed and characterized in the solid-state (**10**•Cu_xBr_y). The outcome serves to highlight that **7** is not as stable as Cu^{I}-NHC complexes with bulky substituents. A single crystal of **10**•$CuBr_2$ was grown from $CHCl_3$ and an X-ray structure determined (Figure 2). X-ray diffraction data of **10**•Br is included in the Supporting Information for comparison. The structure of **10**•$CuBr_2$ shows a $Cu_2Br_4^{2-}$ core with two imidazolium cations. The geometry around each Cu^{I} center is trigonal planar. The NCN face of the imidazolium units are orientated towards the $Cu_2Br_4^{2-}$ core (as a bifurcated H-bond). From separate reactions, a polymorphic form of **10**•Cu_xBr_y was identified by single crystal X-ray diffraction (Figure 3), where the Cu_xBr_y exists as an infinite anionic polymer chain. This X-ray diffraction data set, and indeed another independent set, indicate the presence of a monomeric form of Cu^{I}-NHC **7** within the crystal lattice. The occupancies of these minor species were modelled at 9% and 8% respectively for a Cu^{I} center connected directly to a carbon atom of an NHC ligand (see Supporting Information for details).

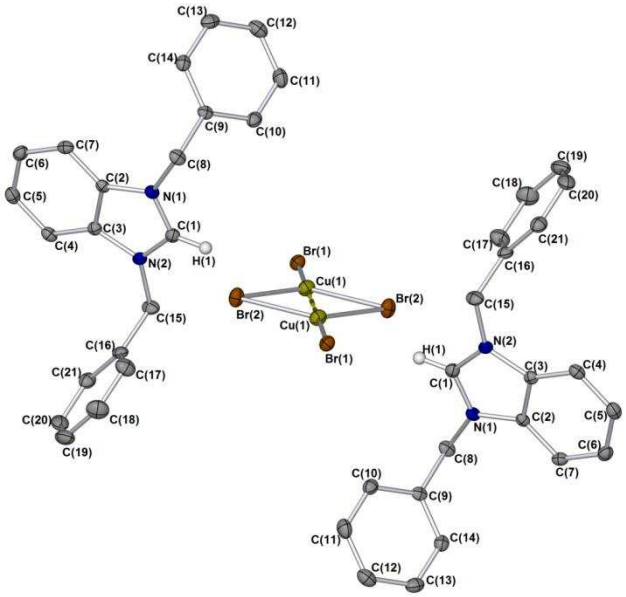

Figure 2. Single crystal X-ray structure of **10**•Cu_2Br_4. Two molecules of $CHCl_3$ are omitted. The Cu-Cu bond distance = 2.8093(4) Å). H1 is the only hydrogen atom shown. Thermal ellipsoids are set to 50% probability.

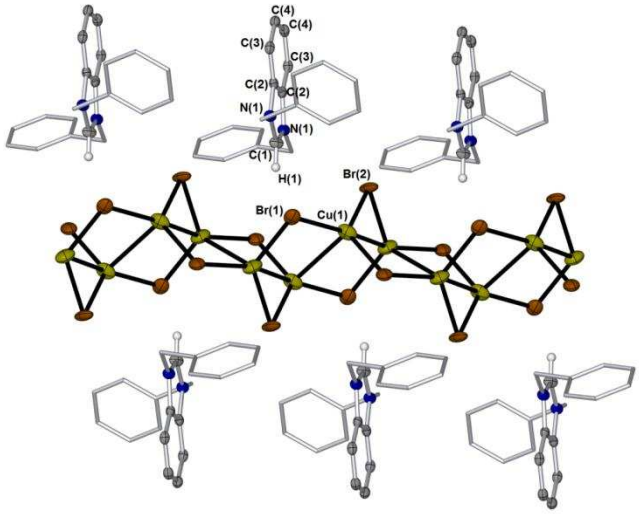

Figure 3. Single crystal X-ray structure of **10**•Cu_xBr_y shown with the 'infinite' polymeric Cu^{I} chain (highlighted by black bonds) surrounded by benzimidazolium cations (6 molecules shown). The benzyl groups are given in stick-form and H1 is the only hydrogen atom shown. Thermal ellipsoids set to 50% probability.

Increasing the volume of solvent (degassed H_2O) and reaction time improved the yield of **7**, aiding Cu_2O solubility, though trace amounts of **10**•Cu_xBr_y were observed by ^{1}H NMR spectroscopic analysis. Complex **7** was therefore prepared by employing the electrochemical procedure developed by Willans and co-workers,[28,29] which produced the desired Cu^{I}-NHC cleanly in 68 % yield.

It was subsequently determined that **10**•Cu_xBr_y was slowly formed from **7**, by addition of D_2O to a CD_3CN solution of **7** (see Supporting Information for details), highlighting a potential competing pathway under the reaction conditions. This indicates that H_2O as a reaction solvent to prepare Cu^{I}-NHCs can be problematic when *N*-substituents with little steric bulk are employed. Our findings may also suggest a pathway for catalyst deactivation for Cu^{I}-NHCs as catalysts in the presence of water, and offer a reason to why high catalyst loadings or stoichiometric quantities are often necessary.[4-14,18]

Cu^{I}-NHC complexes **8** and **9** were prepared by reaction of the corresponding imidazolium salts with Cu_2O in anhydrous DCM (both formed in quantitative yield). Single crystals of complex **8** suitable for X-ray diffraction analysis were grown *via* the vapor diffusion of diethyl ether into a solution of the product in dichloromethane. The molecule crystallizes as a one-dimensional polymer propagated by the formation of bromide bridges (μ^2-Br) along the crystallographic *b*-axis between neighboring NHC-Cu-Br units (Figure 4). Each monomer of the polymer is separated by a distance of 3.89 Å, corresponding to the length of the *b*-axis of the unit cell. Such ligand-unsupported zigzag (metal-halide)$_n$ chains are rare and, to our knowledge, are unprecedented in Cu^{I}-NHC chemistry. This leads to a distorted trigonal planar coordination environment about the Cu^{I} center. π-π Stacking interactions between the phenyl rings are also evident throughout the crystal lattice.

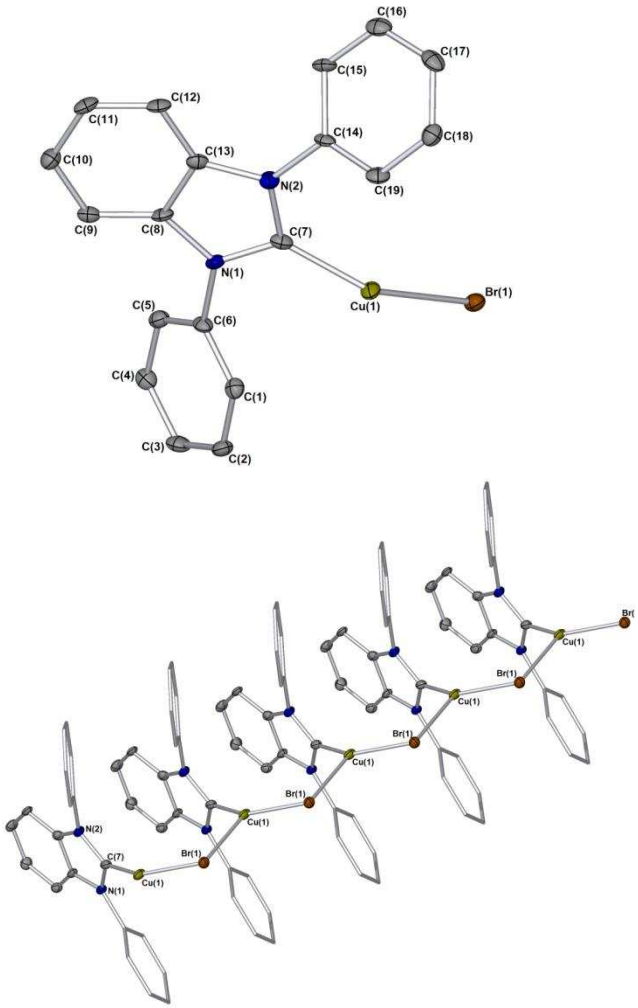

Figure 4. Single crystal X-ray structure of **8**. Hydrogen atoms are omitted for clarity. Thermal ellipsoids are set to 50% probability. The bottom image shows the polymer-like structure which extends throughout the crystal lattice.

Reaction of Cu^{I}-NHC complexes 7-9 with PhI, with and without $Pd(OAc)_2$. Reactions of NHCs with activated and electron-deficient (hetero)aryl halides have been of interest since the early work of Arduengo *et al.*, who showed that an imidazol-2-ylidene in the presence of iodopentafluorobenzene (C_6F_5I) is in equilibrium with an iodoimidazolium adduct (Scheme 3a).[30] Arnold *et al.* studied a more structurally complex system resulting in cleavage of the C-I bond in C_6F_5I, leading to C-I bond formation at the carbene carbon.[31] However, no reaction was noted with PhI, which contains a slightly stronger C-I bond. On the other hand, Henkel *et al.* observed displacement of the 4-fluoro substituent in perfluoropyridine by an imidazol-2-ylidene (Scheme 3b).[32] We have mentioned earlier that aryl and NHC ligands can reductively eliminate at Ni^{II} and Pd^{II} to give 2-arylated imidazolium salts.[22,24,25]

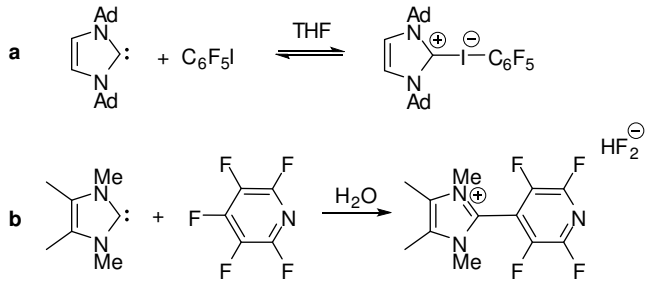

Scheme 3. Examples of previous work assessing the reactivity of NHCs toward aryl halides in the absence of a transition metal.[30,32]

To unequivocally address whether Cu^{I}-NHCs **7-9** can enter into a reaction with PhI, reactions of Cu^{I}-NHCs with PhI were conducted in benzene at 90 °C, in the absence (conditions A) and presence (conditions B) of $Pd(OAc)_2$ (Scheme 4). The reagents were added to a Young's NMR tube under anhydrous conditions, heated at 90 °C, and followed by ^{1}H NMR spectroscopy. The benzyl methylene protons in compound **7** provide a good handle to follow this particular reaction, shifting upfield by 0.15 ppm on going from starting material **7** to product **11** (Figure 5). After 24 hours, the benzene was removed from the reaction *in vacuo* and the reaction mixture was analyzed in CD_3CN to enable direct comparison with authentic starting material and product. Spectrum c shows the outcome of the reaction of compound **7** with ArI under conditions A (Figure 5). Three species were observed in the ^{1}H NMR spectrum at δ 5.69 (Cu^{I}-NHC **7**), δ 5.54 (arylated product **11**) and δ 5.09 (1,3-dibenzyl-2-benzimidazolone). The formation of imidazolone compounds in Cu^{I}-NHC chemistry has been observed previously, and is thought to occur due to trace oxygen in the reaction.[33] ESI-MS revealed the presence of ions at *m*/*z* 299, which is the 1,3-dibenzylbenzimidazolium cation derived from **7**, and *m*/*z* 375, which is the arylated product **11**. Thus, the NHC in compound 7 has undergone arylation in the absence of $Pd(OAc)_2$ at 31% conversion to **11** after 24 h (by ^{1}H NMR). The formation of 1,3-dibenzyl-2-benzimidazolone was recorded in 15%, with 54% of starting material **7** remaining.

The same reaction in the presence of $Pd(OAc)_2$ (1 eq.) was carried out, with ^{1}H NMR spectroscopy (Figure 5d) showing a new species at δ 5.54 (arylated product **11**; 43% conv. by ^{1}H NMR), and ESI-MS showing only *m*/*z* 375 (*i.e.* compound **11**). In this latter reaction, two other species are also present in the ^{1}H NMR spectrum, an AB quartet centered at δ 5.9 ($^2J_{HH}$ ~17 Hz), and a singlet at δ 5.09 (1,3-dibenzyl-2-benzimidazolone; 6% conv.). The AB quartet is attributable to a *cis*-$Pd(NHC)_2Br_2$ complex (Figure 6), with the diastereotopy determined by molecular symmetry, *i.e.* the two NHC ligands are in a *cis*-arrangement. The *cis*-$Pd(NHC)_2Br_2$ complex was recorded in 51% conversion (by ^{1}H NMR). This observation provides evidence that, in the presence of $Pd(OAc)_2$, the Cu^{I}-NHC acts as a transmetallating agent, with arylation likely occurring from Pd.

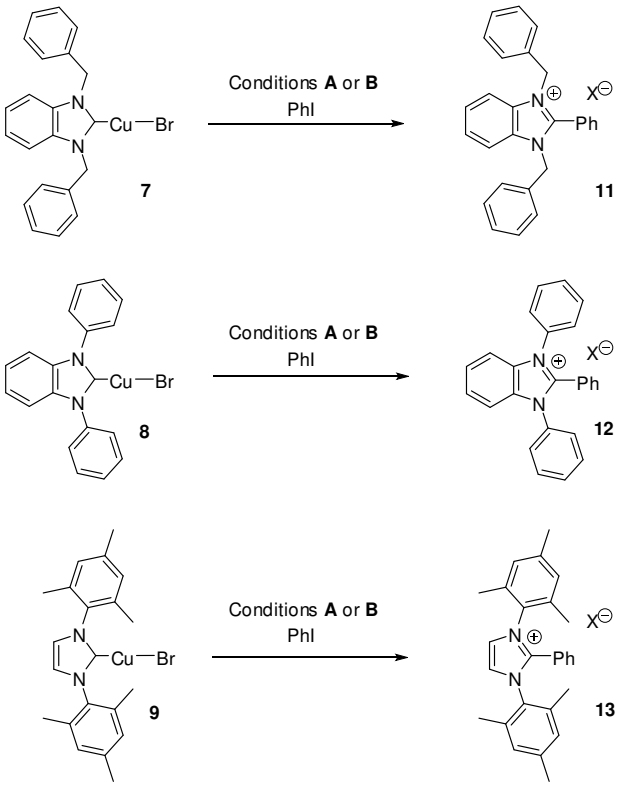

Scheme 4. Assessing the reactivity of Cu^{I}-NHCs toward PhI. Conditions A: PhI (5 eq.), C_6H_6, 90 °C, 24 h. Conditions B: PhI (5 eq.), $Pd(OAc)_2$ (1 eq.), C_6H_6, 90 °C, 24 h. Note that the anion is likely CuX_2 or Cu_2X_4 anions (where X = Br or I).

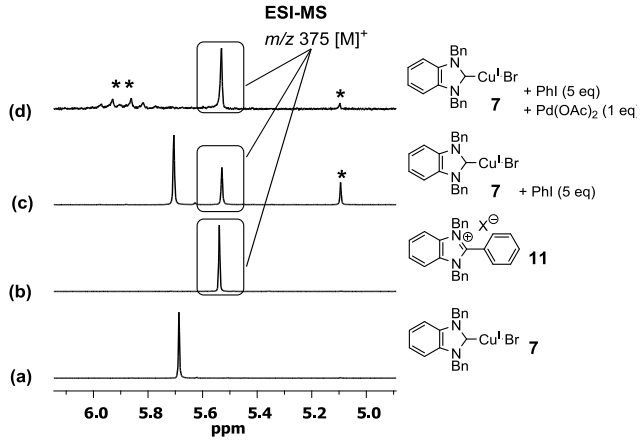

Figure 5. ^{1}H NMR spectra showing reaction outcome of Cu^{I}-NHC **7** with PhI, showing reaction outcome of CuI-NHC **7** with PhI, in the absence (c, conditions A) and presence (d, conditions B) of $Pd(OAc)_2$ (in CD_3CN). Reference spectra shown in (a) **7** and (b) **11** (X anion = $CuBr_2$ or CuI_2). * = 1,3-dibenzyl-2-benzimidazolone. ** = $Pd(NHC)_2Br_2$.

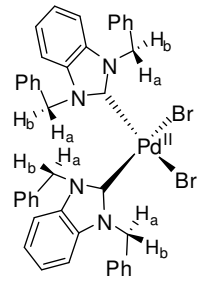

Figure 6. Postulated structure of *cis*-$Pd(NHC)_2Br_2$ obtained from the transmetallation reaction of $Pd(OAc)_2$ with complex **7** in benzene.

The reaction of iodobenzene with Cu^{I}-NHC complexes **8** and **9** was performed under similar reaction conditions as described above for complex **7**. The depletion of complex **8** can be monitored by ^{1}H NMR spectroscopic analysis in C_6D_6, with the product (**12**) precipitating from solution as a white solid. In the presence of $Pd(OAc)_2$, arylation was found to proceed with complex **8** at 90 °C, with starting complex **8** being fully consumed after 2 hours. The arylated imidazolium product **12** precipitated from solution in quantitative yield (isolated yield = >99%). In the absence of $Pd(OAc)_2$ a similar outcome was recorded, with quantitative conversion to **12** after 24 hours. A single crystal of **12** was grown from acetonitrile and the solid-state structure determined using X-ray diffraction analysis (Figure 7). The unit cell contains four cations (two of which are related to the other two by inversion), with each positively-charged arylated imidazolium species being charge balanced by a Cu^{I}-containing $Cu_2I_4^{2-}$ anion. The bonds connecting the phenyl moieties to the imidazolium rings were measured as 1.480(7) and 1.472(7) Å for C(7)-C(8) and C(32)-C(33) respectively. The bond angles around N(2)-C(7)-C(8) and N(3)-C(32)-N(33) are 126.2(5) and 127.8(5)° respectively. The N(2)-C(7)-C(8)-C(9) and N(3)-C(32)-C(33)-C(38) torsion angles lie at 63.8(8) and 68.5(7)° respectively.

When studying reactions with complex **8** at room temperature (rather than heating to 90 °C), a different outcome was recorded. Whilst no reaction was observed in the absence of $Pd(OAc)_2$, in the presence of $Pd(OAc)_2$ *trans*-$[Pd(NHC)\text{-}\kappa^1\text{-}Br\text{-}\mu_2\text{-}Br]_2$ was formed quantitatively (as shown by ^{1}H NMR spectroscopic analysis). Single crystals of the Pd-NHC complex were grown *via* slow evaporation from dichloromethane. The structure shows a dinuclear Pd^{II}-NHC complex, with each Pd^{II} center being coordinated by one *N*-heterocyclic carbene, one terminal bromide atom and two μ-bromide atoms (Figure 8). The C(1)-Pd(1) and C(20)-Pd(2) bond distances were measured at 1.941(6) and 1.931(6) Å respectively, which are comparable to other Pd-NHC complexes exhibiting bridging bromide atoms in the solid-state.[34] The *trans*-C(1)-Pd(1)-Br(2) angle is 176.56(17)° and C(20)-Pd(2)-Br(1) is 176.44(16)°.

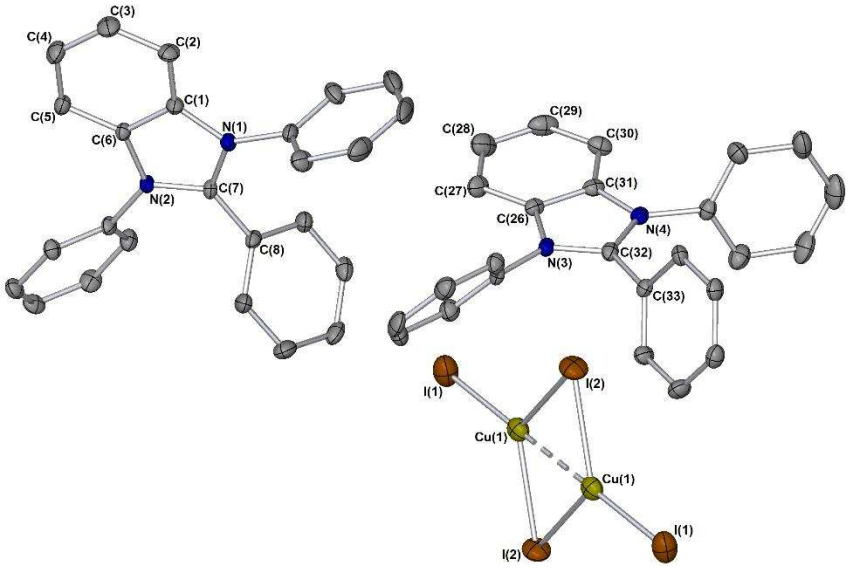

Figure 7. Single crystal X-ray structure of **12** (two independent organic fragments accompany the $Cu_2I_4^{2-}$ anion shown in the figure above). Hydrogen atoms are omitted for clarity. Thermal ellipsoids are set to 50% probability.

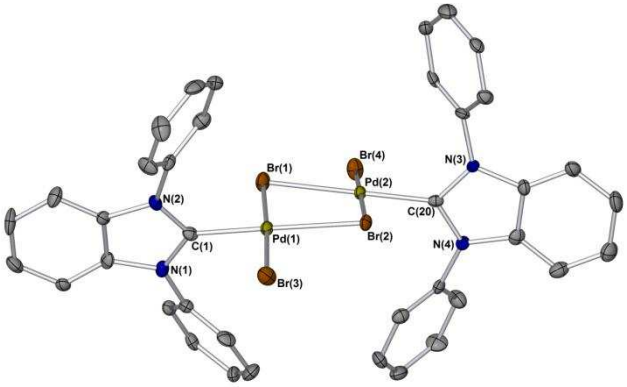

Figure 8. Single crystal X-ray structure of *trans*-$[Pd(NHC)\text{-}\kappa^1\text{-}Br\text{-}\mu_2\text{-}Br]_2$. Hydrogen atoms are omitted for clarity. Thermal ellipsoids are set to 50% probability.

Under reaction conditions **A** (90 °C, 24 h, in the absence of $Pd(OAc)_2$), arylation did not occur with *N*-mesityl substituted Cu^I-NHC complex **9**. In the presence of $Pd(OAc)_2$, a complex mixture of compounds was formed, for which characterization was not possible.

Considering the *a*-values (describing steric effects for various substituents) for benzyl and phenyl groups, the phenyl group is considerably larger (Bn = 1.35 and Ph = 3).[35] It is therefore surprising that arylation occurs in higher yield for the *N*-phenyl derivative (**8**→**12**). Increasing the steric bulk further to *N*-mesityl hinders the arylation reaction. This indicates that the electronic effects of the *N*-substituent also have an influence on the arylation reaction

DFT calculations – assessment of the reaction pathway for arylation in the absence of Pd. As the direct reaction of Cu^I-NHC with iodobenzene to give arylated products is feasible (reactivity order **8** > **7** >> **9**), density functional theory (DFT) was used to understand potential reaction pathways for this process. The first pathway considered was a carbene insertion mechanism (*via* **I**, Scheme 5), akin to that reported by Pérez *et al.*[36] A second pathway involves a Cu^I/Cu^{III} oxidative addition/reductive elimination cycle (*via* **II** and **II'**), as suggested by Ribas *et al.* in other systems.[37,38]

To better understand the feasibility of some of these mechanistic proposals, in addition to the effect of the steric bulk of the *N*-substituent on reactivity, DFT calculations were conducted at the Mo6 level of theory for different NHC ligands (L); for the benzoimidazolin-2-ylidene system where R = benzyl (Bn) and phenyl (Ph), and imidazolin-2-ylidene where R = mesityl (Mes).

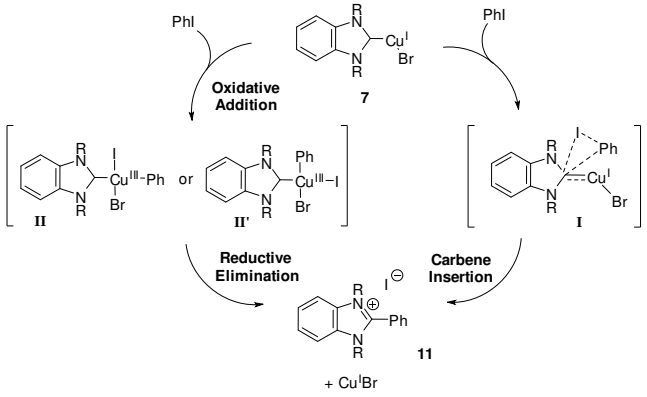

Scheme 5. Mechanistic pathways considered by DFT.

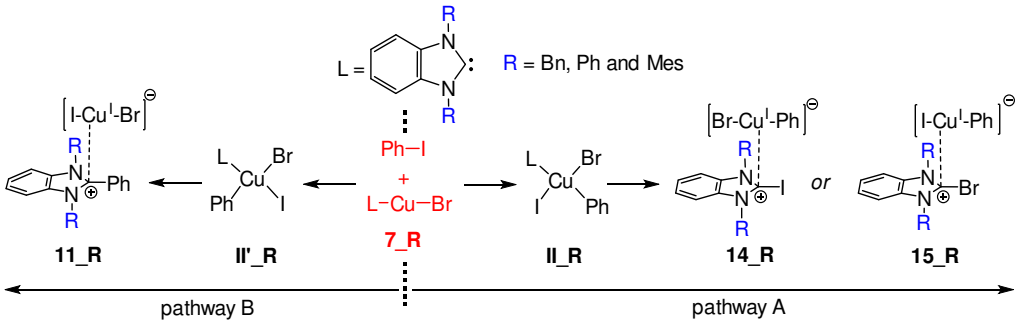

Figure 9. Pathways for the reaction of Cu^{I}-NHC with PhI to form halo-imidazolium (pathway A) or phenyl-imidazolium salts (pathway B).

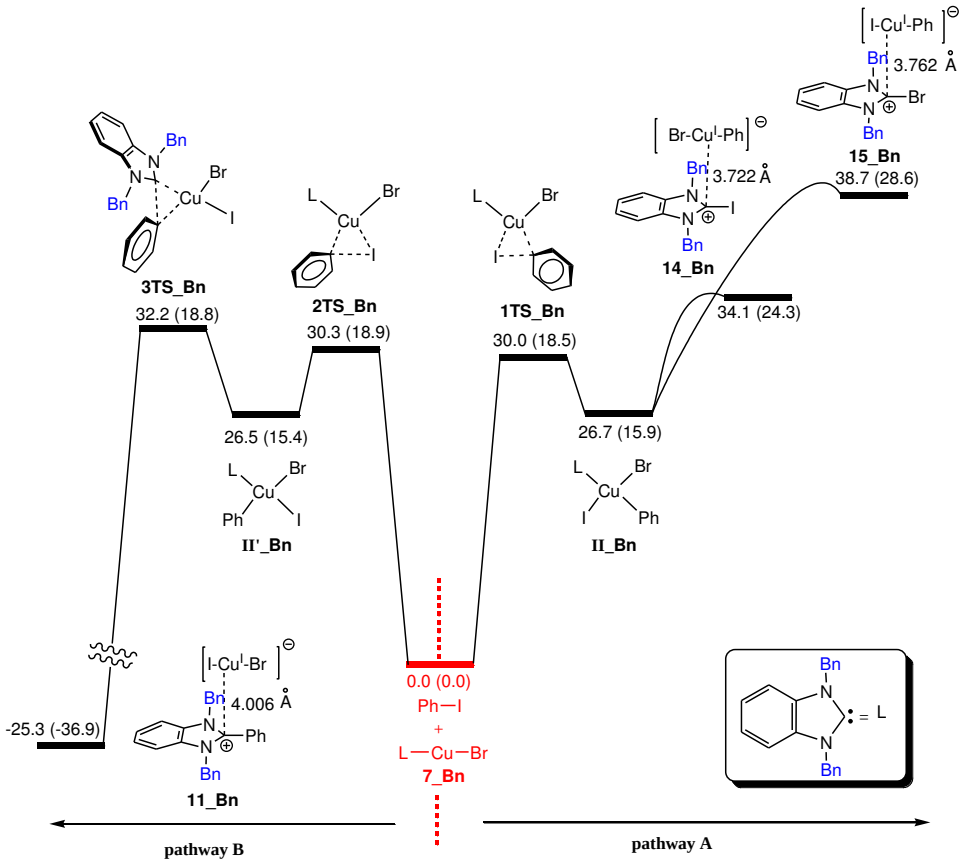

Figure 10. The calculated energy profile for C-I, C-Br and C-C couplings starting from **7_Bn** + PhI *via* the oxidative addition/reductive elimination mechanism. The relative Gibbs energies and electronic energies (in parentheses) obtained from the M06/BS2//B3LYP/BS1 calculations in toluene are given in kcal mol^{-1}.

Initial calculations revealed that the carbene insertion pathway was unfeasible. Indeed, the oxidative addition/reductive elimination sequence was found to be most likely. For example, iodobenzene can oxidatively add to Cu^{I} to give two different Cu^{III} isomers, **II_R** and **II'_R**, where the former has a phenyl group that is *trans* to the NHC ligand and the latter where the phenyl group is *cis* to the NHC ligand (Figure 9). Interestingly, the two intermediate species (**II_R** and **II'_R**) were computed to be competitive. Crucially, the oxidative addition reactions are endergonic, which supports the fact that the oxidation state of +3 at copper is unstable.

The intermediate **II_R** can undergo the C-I (or C-Br) reductive elimination process to produce **14_R** or **15_R** (Figure 9, pathway A), as both bromide and iodide ligands are *cis* to the NHC ligand. The formation of halo-imidazolium salts from Cu-NHCs has recently been reported by Willans and co-workers, with the presence of a Cu^{II}-NHC and excess $CuBr_2$ appearing to drive the successive disproportionation and reductive elimination reaction.[39] In the case of this work, calculations indicate that the C-I (or C-Br) couplings are energetically unfavorable (shown in Figure 10 for R = Bn and Supporting Information for R = Ph and Mes), explaining why the C-I and C-Br couplings are not observed experimentally under the conditions described earlier. By contrast, the intermediate **II'_R** (Figure 9, pathway B) can undergo the C-C reductive elimination to produce the initial product **11_R**. The corresponding reaction is entirely exergonic and has a small activation barrier ranging from 2.8 kcal/mol for R = Ph to 6.0 kcal/mol for R = Mes (Figure 11).

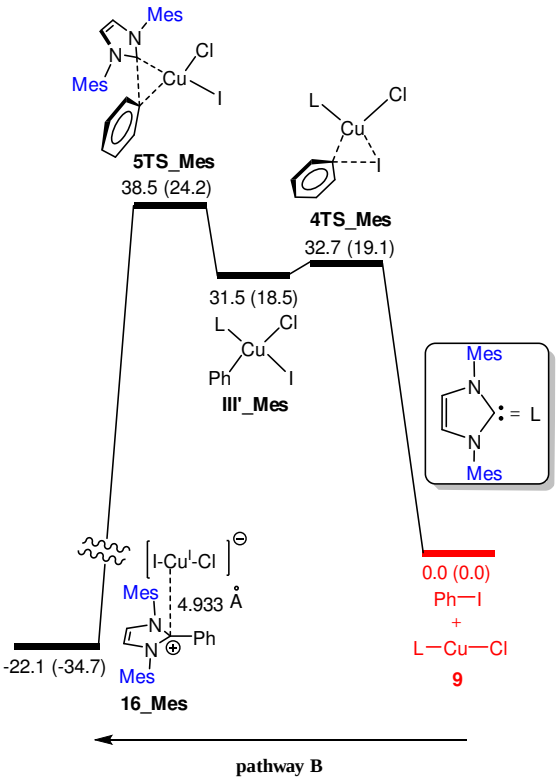

Figure 11. The calculated energy profile for C-C coupling starting from **9** + PhI *via* the oxidative addition/reductive elimination mechanism. The relative Gibbs energies and electronic energies (in parentheses) obtained from the M06/BS2//B3LYP/BS1 calculations in toluene are given in kcal mol^{-1}.

Interestingly, the stability of **II'_R** is affected by the steric bulk of the R groups; for the less bulky R groups such as Bn, and Ph, intermediate **II'_R** is relatively stable (Figure 12) and as a result the C-C reductive elimination reactions can occur with overall energy barriers being accessible under the reaction conditions; 32.2 and 27.5 kcal/mol for R = Bn and Ph, respectively. For comparability, we also computed a pathway for the hypothetical compound, where R = Mes (green pathway in Figure 12). In this case the C-C reductive elimination requires an overall activation barrier of 39.4 kcal/mol, which is too high in energy. This is presumably due to the steric bulk of the Mes groups decreasing the stability of intermediate **II'_Mes**, in turn, leading to an increase in the overall activation barrier of the C-C reductive elimination reaction.

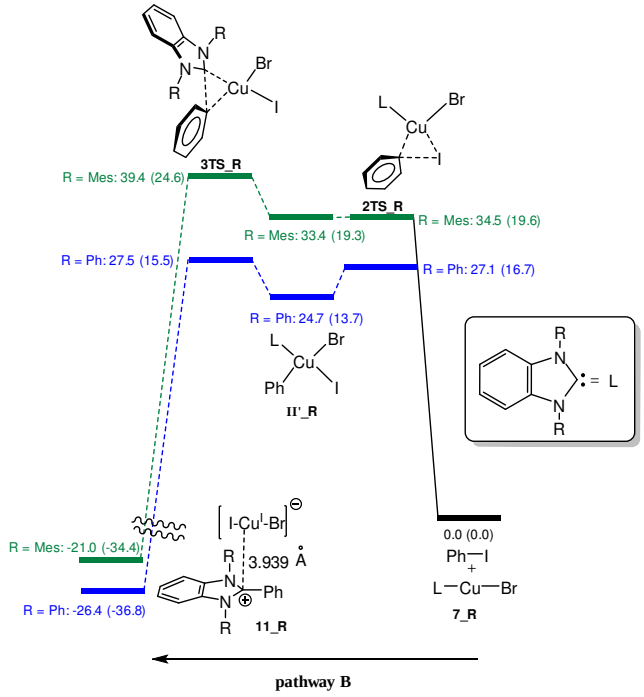

Figure 12. The calculated energy profile for C-C couplings starting from **7_R** + PhI (R = Ph and Mes) *via* the oxidative addition/reductive elimination mechanism (where R = Mes, this has been included for comparison from a theoretical perspective). The relative Gibbs energies and electronic energies (in parentheses) obtained from the M06/BS2//B3LYP/BS1 calculations in toluene are given in kcal mol^{-1}. See supporting information for complete energy landscapes (similar to Fig. 10).

The DFT calculations show that the Cu-$C_{carbenic}$ bonds are lengthened upon going from **7_R** to **II'_R** (Figure 13) . Although, the lengthening of the Cu-$C_{carbenic}$ bond for the cases of R = Bn (0.039 Å) and R = Ph (0.043 Å) is comparable, it is more significant where R = Mes (0.118 Å). This result suggests that the steric hindrance of the mesityl groups renders the Cu-$C_{carbenic}$ bond in **II'_Mes** significantly weak, thereby leading to increased destabilization of **II'_R** relative to **7_R**, ultimately diminishing the reactivity of **7_Mes**.

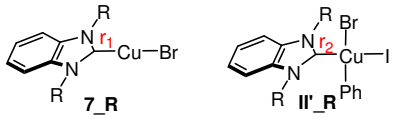

R	r_1(Å)	r_2(Å)	$\Delta r = r_2 - r_1$
Bn	1.933	1.972	0.039
Ph	1.933	1.976	0.043
Mes	1.925	2.043	0.118

Figure 13. The calculated Cu-C(NHC) bond distances for **7_R** (r_1) and **II'_R** (r_2) and the Cu-C(NHC) distance variations (Δr) upon moving from **7_R** to **II'_R**.

Our calculations at the M06/BS2 level predict that **7_Ph** with an activation energy of 27.5 (15.5) kcal/mol is more reactive than **7_Bn** with an activation energy of 32.2 (18.8) kcal/mol. The difference in reactivity cannot be explained in terms of the steric effects. The stabilizing dispersive interaction between *N*-phenyl substituents and Cu-bound phenyl group in **3TS_Ph** is most likely the reason for this difference. Given that B3LYP suffers from the *lack of* dispersion effect, the single point calculations using the B3LYP/BS2 level can help to further support this claim. In contrast to the M06 calculation, the B3LYP predicts that the reactivity of **7_Ph** and **7_Bn** should be comparable; the relative energy of **3TS_Ph** and **3TS_Bn** *at* the B3LYP level are calculated to be 37.5 (25.5) and 37.9 (24.5) kcal/mol, respectively. This result confirms the assumption that the higher reactivity obtained for **7_Ph** at the M06 level is due to the dispersive interactions in **3TS_Ph**.

On the carbene insertion pathway: the transition state for the insertion mechanism is not a stationary point on the PES and all attempts to locate it led to the transition structure **2TS_R**. This is mainly due to the barrier for this process being inaccessibly high. Our calculations showed that the transition state for the insertion mechanism is at least 20 kcal/mol higher in energy than the transition structure **2TS_R**.

The reaction with Pd^{II} (*i.e.* in the presence of $Pd(OAc)_2$) involves transmetallation of the NHC ligand from $Cu^{I} \rightarrow Pd^{II}$, which is well established. Indeed, as noted earlier, the arylation[22-24] and alkylation[26] of NHC ligands at Pd^{II} are reported.

Conclusion

In conclusion, Cu^{I}(NHC)Br complexes (**7** and **8**) undergo a direct reaction with iodobenzene to give 2-arylated benzimidazolium products, **11** and **12** respectively. The nature of the *N*-substituent on the NHC ligand influences the reactivity of the Cu^{I}(NHC)X complex towards arylation. *N*-Benzyl (**7**) or *N*-phenyl (**8**) substituents facilitate arylation, whereas *N*-mesityl substituents (**9**) hinder the arylation reaction. The less hindered Cu^{I}(NHC)Br complex (**7**), with *N*-benzyl substituents, is susceptible to oxidation reactions to afford 1,3-dibenzylbenzimidazolium cations containing a $Cu_x^{I}Br_y$ anion (**10**, including various polymorphs).

The reaction of **7** with iodobenzene is aided by $Pd(OAc)_2$, where a transmetallation product, *cis*-$Pd(NHC)_2Br_2$, was characterized spectroscopically. In the case of **8**, a related transmetallation product was formed in reactions conducted at room temperature, namely *trans*-[Pd(NHC)-κ^1-Br-μ_2-Br]$_2$, confirmed by single crystal X-ray diffraction. More generally these findings confirm that Cu^{I}(NHC)X complexes are viable intermediates of relevance to the C-H bond functionalization of (benz)azoles at both Cu and Pd.

Finally, Density Functional Theory calculations have shown that an oxidative addition/reductive elimination pathway, involving Cu^{III} species, is an energetically feasible process. Future mechanistic studies will examine whether Cu^{III} intermediates in the Cu-assisted C-H bond functionalization of heteroarenes can be detected and characterized by X-ray absorption spectroscopic (XAS) analysis under working reaction conditions.

Experimental

General synthetic details. All air sensitive procedures were carried out using Schlenk techniques (high vacuum, liquid nitrogen trap on a standard in-house built dual line). Where necessary a glove (dry) box was used (<0.5 ppm O_2). Room temperature upper and lower limits are stated as 13-25 °C, but typically 21-23 °C was recorded. Commercial chemicals were purchased from Sigma-Aldrich® and Alfa Aesar® and used directly unless otherwise stated in the text. TLC analysis was carried out on Merck TLC aluminium sheets (silica gel 60 F254) and visualized with UV light (at 254 nm), iodine vapour or an aqueous solution of potassium permanganate. Flash chromatography was run on silica gel 60.[40] Melting points were recorded using a Stuart digital SMP3 machine and are uncorrected values. NMR spectra were obtained in the solvent indicated, using a JEOL ECX400 (400 MHz and 101 MHz for ^{1}H and ^{13}C, respectively). Chemical shifts are reported in parts per million and were referenced to the residual non-deuterated solvent of the deuterated solvent used. Spectra were typically run at a temperature of 300 K. All ^{13}C NMR spectra were obtained with ^{1}H decoupling. NMR spectra were processed using MestReNova software (versions 8.01 and 9.01). The spectra given below were saved as either .BMP or .PNG files in MestReNova and inserted directly into a Microsoft Word Document. For the ^{1}H NMR spectra the resolution varies from 0.15 to 0.5 Hz; the coupling constants have been quoted to ±0.5 Hz in all cases for consistency. ^{1}H NMR chemical shifts are quoted to 2 decimal places; ^{13}C NMR chemical shifts are quoted to 1 decimal place. Numbers were rounded to the nearest value, *e.g.* 1.237 ≈ 1.24, 1.232 ≈ 1.23.

MS spectra were measured using a Bruker Daltonics micrOTOF MS, Agilent series 1200LC with electrospray ionisation (ESI and APCI) or on a Thermo LCQ using electrospray ionisation, with <5 ppm error recorded for all HRMS samples. LIFDI mass spectrometry was carried out using a Waters GCT Premier MS Agilent 7890A GC (usually for analysis of organometallic compounds when ESI or APCI are not satisfactory ionisation methods). Mass spectral data is quoted as the *m/z* ratio along with the relative peak height in brackets (base peak = 100).

X-Ray crystallography. For all compounds other than compound 8, diffraction data were collected at 110 K on a Bruker Smart Apex diffractometer with Mo-K_α radiation (λ = 0.71073 Å) using a SMART CCD camera. Diffractometer control, data collection and initial unit cell determination was performed using "SMART" (v5.625 Bruker-AXS). Frame integration and unit-cell refinement software was carried out with "SAINT+" (v6.22, Bruker AXS). Absorption corrections were applied by SADABS (v2.03, Sheldrick). Structures were solved by direct methods using SHELXS-97 (Sheldrick, 1990) and refined by full-matrix least squares using SHELXL-97 (Sheldrick, 1997). All non-hydrogen atoms were refined anisotropically. Hydrogen atoms were placed using a "riding model" and included in the refinement at calculated positions. Data tables for all the X-ray crystal structures reported in this paper can be found in the Supporting Information files. X-ray diffraction data for compound **8** were collected on an Agilent SuperNova diffractometer fitted with an Atlas CCD detector with Cu-K_α radiation (λ = 1.54184 Å). The crystal was mounted under Fomblin on a nylon loop. The crystal

was held at 100 K using an Oxford Cryosystems low temperature device during unit cell determination and data collection. The data set was corrected for absorption effects using a multiscan method, and the structure was solved using SHELXS-97 interfaced through the program X-Seed. Refinement was by full-matrix least squares on F2 using ShelXL-97, interfaced through the program X-Seed. All hydrogen atoms were included at geometrically estimated positions using a riding model.

DFT calculations. Gaussian 09[41] was used to fully optimize all of the structures reported in this paper at the B3LYP level of density functional theory (DFT).[42] The effective core potential of Hay and Wadt with a double-ξ valence basis set (LANL2DZ)[43,44] was chosen to describe Cu and I. The 6-31G(d) basis set was used for other atoms.[45] Polarization functions for Cu(ξ_f = 3.525) and I (ξ_d = 0.289) were also added.[46,47] This basis set combination will be referred to as BS1. Frequency calculations were carried out at the same level of theory as for structural optimization. IRC[48,49] calculations were used to confirm the connectivity between transition structures and minima. Because recent studies have established that M06[50-52] predicts the activation energies more accurately than B3LYP,[53] we carried out single-point energy calculations for all the structures with a larger basis set (BS2) at the M06 level. BS2 utilizes the quadruple-ζ valence def2-QZVP[54] basis set on Cu and the 6-311+G(2d,p) basis set on other atoms. The solvation energies were calculated using BS2 on optimized geometries with the CPCM solvation model using toluene as solvent.[55] To estimate the corresponding Gibbs free energies, ΔG, the entropy corrections were calculated at the B3LYP/BS1 level, adjusted by the method proposed by Okuno[56] and finally added to the M06/BS2 total energies. We have used the potential and Gibbs free energies obtained from the M06/BS2//B3LYP/BS1 calculations in DMF throughout the paper unless otherwise stated.

Cu(benzoNHC-Bn)Br (7). An oven-dried, three-necked, round-bottomed flask was charged with 1,3-dibenzylbenzo[d]imidazolium bromide (389 mg, 1 mmol,) (0.38 g, 1.0 mmol), which was thoroughly dried/degassed *in vacuo*. Anhydrous acetonitrile (15 ml) was cannula transferred in to the flask dissolving the imidazolium salt. The solution was degassed (by bubbling with argon for >1 hour). The two copper electrodes were inserted in to the reaction flask and purged with argon (for > 30 minutes) and then inserted in to the reaction mixture. A potential was applied such that a current of 50 mA flowed through the solution. The solution was electrolysed for 1.5Q. Following electrolysis, the mixture was filtered and the solvent removed from the filtrate in vacuo to yield a pale yellow solid. This was recrystallised twice from dichloromethane / diethyl ether to yield the product as a white crystalline solid. Yield: 0.30 g, 0.68 mmol, 68%.Single crystals suitable for X-ray analysis were grown by vapour diffusion of pentane in to a concentrated dichloromethane solution of the product. ^{1}H NMR (500 MHz, CD_2Cl_2) δ 7.40 – 7.32 (m, 12H, ArH), 7.30 – 7.27 (m, 2H, ArH), 5.69 (s, 4H, 2xCH_2); ^{1}H NMR (400 MHz, MeCN-d_3) δ 7.44 (dd, $^3J_{HH}$ = 6.0, $^3J_{HH}$ = 3.0 Hz, 2H, ArH), 7.39 – 7.25 (m, 12H, ArH), 5.69 (s, 4H, 2xCH_2); ^{13}C{^{1}H} NMR (126 MHz, CD_2Cl_2) δ 135.9, 129.6, 129.0, 128.0, 124.7, 112.5, 53.4 (7 of 9 resonances observed); Anal. calc. for $C_{21}H_{18}BrCuN_2$ C 57.09, H 4.11, N 6.34, observed C 56.90, H 4.05, N 6.15; LIFDI-MS *m/z* (%) 440 (67) [^{63}Cu^{79}BrM] $^{\cdot+}$, 441 (12) [^{63}Cu^{79}Br^{13}CM] $^{\cdot+}$, 442 (100) [^{63}Cu^{81}BrM and ^{65}Cu^{79}BrM] $^{\cdot+}$, 442 (22) [^{63}Cu^{81}Br^{13}CM or ^{65}Cu^{79}Br^{13}CM] $^{\cdot+}$, 443 (28) [^{65}Cu^{81}BrM]$^{\cdot+}$ (observed as monomer only). Additional details on the decomposition of complex **7** in the presence of water and air is given in the Supporting Information file.

Cu(benzoNHC-Ph)Br (8). A Schlenk flask was charged with 1,3-diphenylbenzimidazolium bromide (527 mg, 1.5 mmol), Cu_2O (429 mg, 3 mmol) and 4 Å molecular sieves. These were dried and degassed thoroughly *in vacuo*. Anhydrous CH_2Cl_2 (30 mL) was added *via* cannula and the mixture was stirred at reflux for 24 h. After this time, the mixture was allowed to cool and was removed from the filtrate *in vacuo* to give the product as a white-off solid (99 % yield, 0.449 g). MP: 205-208 °C; ^{1}H NMR (400 MHz, CD_2Cl_2) δ 7.78-7.75 (m, 4H, ArH), 7.70-7.65 (m, 4H, ArH), 7.64-7.60 (m, 2H, ArH), 7.56-7.51 (m, 2H, ArH), 7.48-7.43 (m, 2H, ArH); ^{1}H NMR (400 MHz, CD_3CN) δ 7.77-7.74 (m, 4H, ArH), 7.69-7.60 (m, 6H, ArH), 7.55-7.50 (m, 2H, ArH), 7.48-7.44 (m, 2H, ArH); ^{13}C{^{1}H} NMR (101 MHz, CD_2Cl_2) δ 138.04, 134.61, 130.61, 130.06, 126.60, 125.52, 112.78 (7 of 8 resonance observed); ESI-HRMS *m/z* 603.1616 observed as [Cu(bNHC-Ph)$_2$]$^+$ (calc. for $C_{38}H_{28}CuN_4$ 603.1610); LIFDI-MS *m/z* (%) 603.21 (100) [Cu(bNHC-Ph)$_2$]$^+$, 605.23 (45), 606.23 (18). IR (solid-state ATR, cm^{-1}) 3041, 2962, 1590, 1482, 1357, 1259, 1047, 796, 740, 693, 603, 501. Anal. calc. for $C_{19}H_{14}Br_{1.04}Cu_{1.04}N_2$,C 54.3, H 3.36, N 6.67, observed C 54.3, H 3.43, N 6.95 (estimated ratio of **8** to CuBr of 22:1, 4%).

Cu(IMes)Cl (9).[27] A Schlenk flask was charged with 1,3-bis(2,4,6-trimethylphenyl) imidazolium chloride (511 mg, 1.5 mmol), Cu_2O (429 mg, 3 mmol) and 4Å molecular sieves. These were dried and degassed thoroughly *in vacuo*. Anhydrous CH_2Cl_2 (30 mL) was added *via* cannula and the mixture was stirred at reflux for 24 h. After this time, the mixture was allowed to cool and the solvent was removed *in vacuo* to give the product as a white-off solid (99 % yield). Representative data: ^{1}H NMR (400 MHz, CD_2Cl_2) δ 7.11 (s, 2H, CH=CH), 7.07 (s, 4H, *meta*CH), 2.38 (s, 6H, 2x*para*CH_3), 2.12 (s, 12 H, 2x*ortho*CH_3); ^{13}C{^{1}H} NMR (101 MHz, CD_2Cl_2) δ 140.19, 135.80, 135.36, 129.87, 122.98, 21.44, 18.13 (7 of 8 resonance observed).

Arylation procedure conditions A. To a Young's NMR tube in the glove-box was added a solution of Cu(NHC)Br (**7** or **8**) or Cu(NHC)Cl **9** (0.0145 mmol, 1 eq.) in anhydrous C_6D_6 (0.7 ml) (distilled from Na). A ^{1}H NMR spectrum (400 MHz) was recorded after *ca.* 20 mins. The sample was returned to the glove-box, where PhI (14.7 mg, 0.0724 mmol, 8 μL, 5 eq.) was added. A ^{1}H NMR spectrum was recorded and the sample was then heated to 90 ^{o}C. ^{1}H NMR spectra were recorded at 2 h and 24 h intervals to monitor any chemical change (all spectra recorded in C_6D_6 are shown in the Supporting Information file). The C_6D_6 solvent was removed *in vacuo* to give a brown solid (no mass loss recorded), which was re-dissolved in CD_3CN (for ease of referencing with authentic standards of the potential products), and a ^{1}H NMR spectrum recorded.

Arylation procedure conditions B. To a Young's NMR tube in the glove-box was added a solution of Cu(NHC)Br (**7**, **8** or **9**) (0.0145 mmol, 1 eq.) in anhydrous C_6D_6 (0.7 ml) (distilled from Na). A ^{1}H NMR spectrum (400 MHz) was then recorded. In the glove-box, PhI (14.7 mg, 0.0724 mmol, 8 ul, 5

eq.) was added, followed by a second ^{1}H NMR spectrum. In the glove-box, $Pd(OAc)_2$ (3 mg, 0.0146 mmol, 1 eq.) was added, followed by a third ^{1}H NMR spectrum (all spectra recorded in C_6D_6 are shown in the Supporting Information file). The sample was then heated to 90 ^oC for 24 h. Concomitant Pd black and product precipitation occurred, preventing any further *in situ* spectroscopic analysis. The solvent was removed *in vacuo* to give a brown solid (no mass loss recorded), which was analyzed by ESI-MS. This brown solid was redissolved in CD_3CN (for ease of referencing with authentic standards of the potential products), and a ^{1}H NMR spectrum recorded.

Representative data for (1,3-dibenzyl)-2-phenylbenzo[*d*]imidazolium copper(I) diiodide (11). MP 101-103 ^oC (decomp.); ^{1}H NMR (400 MHz, CD_3CN) δ 7.85-7.74 (m, 3H, ArH), 7.71-7.61 (m, 6H, ArH), 7.38-7.29 (m, 6H, ArH), 7.18-7.09 (m, 3H, ArH), 5.54 (s, 4H, $2xCH_2$); $^{13}C\{^1H\}$ NMR (101 MHz, CD_3CN) 134.5, 134.40, 132.6, 131.2, 130.9, 130.0, 129.6, 128.4, 128.1, 121.7, 115.0, 50.9 (quaternary C2 not observed); ESI-MS *m/z* 375 $[M]^+$; ESI-HRMS *m/z* 375.1854 (calc. for $C_{27}H_{23}N_2$ 375.1856). LC-MS *m/z* shows 375 as the dominant species in the mass spectrum.

Representative data for (1,3-Diphenyl)-2-phenylbenzo[d]imidazolium copper(I) diiodide (12). MP: 274-277 °C; ^{1}H NMR (400 MHz, CD_3CN) δ 7.77-7.72 (m, 2H, ArH), 7.67-7.57 (m, 12H, ArH), 7.51-7.47 (m, 1H, ArH), 7.45-7.42 (m, 2H, ArH), 7.36-7.32 (m, 2H, ArH); $^{13}C\{^1H\}$ NMR (101 MHz, CD_3CN) δ 137.48, 133.86, 133.63, 133.56, 132.17, 132.09, 131.40, 129.84, 129.05, 128.49, 122.11, 114.46; ESI-HRMS *m/z* 347.1552 $[M-X]^+$, (calc. for $C_{25}H_{19}N_2^+$ 347.1543). IR (solid-state ATR, cm^{-1}) 3042, 1591, 1494, 1442, 1166, 1028, 750, 695, 584, 506. Anal. calc. for $C_{25}H_{19}Br_{0.66}CuI_{1.34}N_2$ C 47.40, H 3.02, N 4.42, observed C 47.54, H 2.93, N 4.19 (estimated ratio of $CuBr_2/CuI_2$ anions is *ca.* 0.33/0.67).

ASSOCIATED CONTENT

Supporting Information

Crystallographic information files (CIF) for the single crystal X-ray structures and xyz coordinates from DFT calculations are available, including accompanying data tables. Further characterization data for compounds (*i.e.* representative NMR spectra) are also provided. This material is available free of charge on the World Wide Web at http://pubs.acs.org.

AUTHOR INFORMATION

Corresponding Authors

* Prof I. J. S. Fairlamb, E-mail: ian.fairlamb@york.ac.uk, Dr. C. E. Willans. Email: c.e.willans@leeds.ac.uk, Dr. A. Ariafard, E-mail: alireza.ariafard@utas.edu.au.

ACKNOWLEDGMENT

We are grateful to the Royal Society for research fellowships (C.E.W. Dorothy Hodgkin fellowship; I.J.S.F. a University Research Fellowship). EPSRC are acknowledged for funding a PhD project (T.J.W.) *via* the DTG scheme (grant code EP/P505178/1). BP UK are acknowledged for providing PhD funding (B.R.M.L.). A.A. thanks the Australian Research Council for financial support, and the Australian National Computational Infrastructure and the University of Tasmania for computing resources.

REFERENCES

1. McGlacken, G. P.; Bateman, L. M. *Chem. Soc. Rev.* **2009**, *38*, 2447-2464.
2. Ackermann, L.; Vicente, R.; Kapdi, A. R. *Angew. Chem. Int. Edit.* **2009**, *48*, 9792-9826.
3. (a) De Ornellas, S.; Storr, T. E.; Williams, T. J.; Baumann, C. G.; Fairlamb, I. J. S. *Curr. Org. Synth.* **2011**, *8*, 79-101. (b) Gayakhe, V.;, Sanghvi, Y. S.; Fairlamb, I. J. S.; Kapdi, A. R. *Chem. Commun.* **2015**, DOI: 10.1039/c5cc03416g.
4. Bellina, F.; Rossi, R. *Adv. Synth. Catal.* **2010**, 352, 1223-1276.
5. (a) Bellina, F.; Cauteruccio, S.; Rossi, R. *Curr. Org. Chem.* **2008**, *12*, 774-790. For a very recent review, see: (b) Hirano, K.; Miura, M. *Top. Catal.* **2014**, *57*, 878-889. For a review of Cu-NHCs in catalysis, see: (c) Egbert J. D.; Cazin, C. S. J.; Nolan, S. P. *Catal. Sci. Tech.* **2013**, *3*, 912-926.
6. Bellina, F.; Cauteruccio, S.; Mannina, L.; Rossi, R.; Viel, S. *J. Org. Chem.* **2005**, *70*, 3997-4005.
7. Bellina, F.; Cauteruccio, S.; Mannina, L.; Rossi, R.; Viel, S. *Eur. J. Org. Chem.* **2006**, 693-703.
8. Bellina, F.; Cauteruccio, S.; Rossi, R. *Eur. J. Org. Chem.* **2006**, 1379-1382.
9. Bellina, F.; Cauteruccio, S.; Rossi, R. *J. Org. Chem.* **2007**, *72*, 8543-8546.
10. Bellina, F.; Calandri, C.; Cauteruccio, S.; Rossi, R. *Tetrahedron* **2007**, *63*, 1970-1980.
11. Bellina, F.; Cauteruccio, S.; Di Fiore, A.; Rossi, R. *Eur. J. Org. Chem.* **2008**, 5436-5445.
12. Bellina, F.; Cauteruccio, S.; Di Fiore, A.; Marchetti, C.; Rossi, R. *Tetrahedron* **2008**, *64*, 6060-6072.
13. Storr, T. E.; Firth, A. G.; Wilson, K.; Darley, K.; Baumann, C. G.; Fairlamb, I. J. S. *Tetrahedron* **2008**, *64*, 6125-6137.
14. Storr, T. E.; Baumann, C. G.; Thatcher, R. J.; De Ornellas, S.; Whitwood, A. C.; Fairlamb, I. J. S. *J. Org. Chem.* **2009**, *74*, 5810-5821.
15. (a) Yoshizumi, T.; Tsurugi, H.; Satoh, T.; Miura, M. *Tetrahedron Lett.* **2008**, *49*, 1598-1600. (b) Pivsa-Art, S.; Satoh, T.; Kawamura, Y.; Miura, M.; Nomura, M. *Bull. Chem. Soc.. Jpn.* **1998**, *71*, 467-473. It is interesting to note the recent publication of a cooperative Pd-Cu direct arylation reaction, see: (c) Lesieur, M.; Lazreg, F.; Cazin, C. S. J. *Chem. Commun.* **2014**, *50*, 8927-8929. It is also important to recognize that transmetallation from CuNHCs to other metal salts is well known, see also: (d) Venkatachalam, G.; Heckenroth, M.; Neels, A.; Albrecht, M. *Helv. Chim. Acta.* **2009**, *92*, 1034. (e) Furst, M. R. L.; Cazin, C. S. J. *Chem. Commun.* **2010**, *46*, 6924.
16. Tan, K. L.; Bergman, R. G.; Ellman, J. A. *J. Am. Chem. Soc.* **2002**, *124*, 3202-3203.
17. Lewis, J. C.; Wiedemann, S. H.; Bergman, R. G.; Ellman, J. A. *Org. Lett.* **2004**, *6*, 35-38.
18. Baumann, C. G.; de Ornellas, S.; Reeds, J. P.; Storr, T. E.; Williams, T. J.; Fairlamb, I. J. S. *Tetrahedron* **2014**, *70*, 6174-6187.
19. de Vries, J. G. *Dalton Trans.* **2006**, 421-429.
20. Reetz, M. T.; de Vries, J. G. *Chem. Commun.* **2004**, 1559-1563.
21. (a) Brackemeyer, D.; Herve, A.; Brinke, C. S. T.; Jahnke, M. C.; Hahn, F. E. *J. Am. Chem. Soc.* **2014**, *136*, 7841-7844. A cluster series of papers, concerning stable carbenes, has been reported, see: (b) Rovis, T. and Nolan, S.P. *Synlett* **2013**, 1188-1189. For related work, see (c) Kösterke, T.; Pape, T.; Hahn, F. E. *J. Am. Chem. Soc.* **2011**, *133*, 2112-2115. (d) Kösterke, T.; Pape, T.; Hahn, F. E. *Chem. Commun.* **2011**, *47*, 10773-10775. (e) Kösterke, T.; Kösters, J.; Würthwein, E.-U.; Mück-Lichtenfeld, C.; Schulte to Brinke, C.; Lahoz, F.; Hahn, F. E. *Chem. Eur. J.* **2012**, *18*, 14594-14598. (f) Das, R.; Daniliuc, C. G.; Hahn, F. E. *Angew. Chem. Int Ed.* **2014**, *53*, 1163-1166. (g) Das, R.; Hepp, A.; Daniliuc, C. G.; Hahn, F. E. *Organometallics* **2014**, *33*, 6975-6987.

22. Graham, D. C.; Cavell, K. J.; Yates, B. F. *Dalton Trans.* **2006**, 1768-1775.
23. Caddick, S.; Geoffrey, F.; Cloke, N.; Hitchcock, P. B.; Leonard, J.; Lewis, A. K. D.; McKerrecher, D.; Titcomb, L. R. *Organometallics* **2002**, *21*, 4318-4319.
24. McGuinness, D. S.; Cavell, K. J.; Skelton, B. W.; White, A. H. *Organometallics* **1999**, *18*, 1596-1605.
25. McGuinness, D. S.; Mueller, W.; Wasserscheid, P.; Cavell, K. J.; Skelton, B. W.; White, A. H.; Englert, U. *Organometallics* **2002**, *21*, 175-181.
26. McGuinness, D. S.; Saendig, N.; Yates, B. F.; Cavell, K. J. *J. Am. Chem. Soc.* **2001**, *123*, 4029-4040.
27. Citadelle, C. A.; Le Nouy, E.; Bisaro, F.; Slawin, A. M. Z.; Cazin, C. S. J. *Dalton Trans.* **2010**, *39*, 4489-4491.
28. Lake, B. R. M.; Bullough, E. K.; Williams, T. J.; Whitwood, A. C.; Little, M. A.; Willans, C. E. *Chem. Commun.* **2012**, *48*, 4887-4889.
29. Bullough, E. K.; Little, M. A.; Willans, C. E. *Organometallics* **2013**, *32*, 570-577.
30. Arduengo, A. J.; Kline, M.; Calabrese, J. C.; Davidson, F. *J. Am. Chem. Soc.* **1991**, *113*, 9704-9705.
31. Arnold, P. L.; Turner, Z. R.; Bellabarba, R.; Tooze, R. P. *J. Am. Chem. Soc.* **2011**, *133*, 11744-11756.
32. Kuhn, N.; Fahl, J.; Boese, R.; Henkel, G. *Z. Naturforsch. (B)* **1998**, *53*, 881-886.
33. Shtyrlin, V. G.; Serov, N. Y.; Islamov, D. R.; Konkin, A. L.; Bukharov, M. S.; Gnezdilov, O. I.; Krivolapov, D. B.; Kataeva, O. N.; Nazmutdinova, G. A.; Wendler, F. *Dalton Trans.* **2014**, *43*, 799-805.
34. Huynh, H. V.; Han, Y.; Ho, J. H. H.; Tan, G. K. *Organometallics* **2006**, *25*, 3267-3274.
35. Anderson, J. E. *J. Chem. Soc.-Perkin Trans. 2* **1974**, 10-13.
36. Caballero, A.; Despagnet-Ayoub, E.; Mar Diaz-Requejo, M.; Diaz-Rodriguez, A.; Elena Gonzalez-Nunez, M.; Mello, R.; Munoz, B. K.; Ojo, W.-S.; Asensio, G.; Etienne, M.; Perez, P. J. *Science* **2011**, *332*, 835-838.
37. Casitas, A.; King, A. E.; Parella, T.; Costas, M.; Stahl, S. S.; Ribas, X. *Chemical Science* **2010**, *1*, 326-330.
38. Casitas, A.; Canta, M.; Sola, M.; Costas, M.; Ribas, X. *J. Am. Chem. Soc.* **2011**, *133*, 19386-19392.
39. Lake, B. R. M.; Ariafard, A.; Willans, C. E. *Chem.-Eur. J.* **2014**, *20*, 12729-12733.
40. Still, W. C.; Kahn, M.; Mitra, A. *J. Org. Chem.* **1978**, *43*, 2923-2925.
41. Firsch, M. J., Gaussian 09 2009, revision A.02; Gaussian, Inc.: Wallingford, CT.
42. Lee, C. T.; Yang, W. T.; Parr, R. G. *Phys. Rev. B* **1988**, *37*, 785-789.
43. Hay, P. J.; Wadt, W. R. *J. Chem. Phys.* **1985**, *82*, 270-283.
44. Wadt, W. R.; Hay, P. J. *J. Chem. Phys.* **1985**, *82*, 284-298.
45. Harihara.Pc; Pople, J. A. *Theor. Chim. Acta* **1973**, *28*, 213-222.
46. Ehlers, A. W.; Bohme, M.; Dapprich, S.; Gobbi, A.; Hollwarth, A.; Jonas, V.; Kohler, K. F.; Stegmann, R.; Veldkamp, A.; Frenking, G. *Chem. Phys. Lett.* **1993**, *208*, 111-114.
47. Hollwarth, A.; Bohme, M.; Dapprich, S.; Ehlers, A. W.; Gobbi, A.; Jonas, V.; Kohler, K. F.; Stegmann, R.; Veldkamp, A.; Frenking, G. *Chem. Phys. Lett.* **1993**, *208*, 237-240.
48. Fukui, K. *J. Phys. Chem.* **1970**, *74*, 4161-4163.
49. Fukui, K. *Acc. Chem. Res.* **1981**, *14*, 363-368.
50. Zhao, Y.; Schultz, N. E.; Truhlar, D. G. J. *Chem. Theor. Comput.* **2006**, *2*, 364-382.
51. Zhao, Y.; Truhlar, D. G. *J. Chem. Phys.* **2006**, *125*, 194101/1-194101/18.
52. Zhao, Y.; Truhlar, D. G. *J. Phys. Chem. A* **2006**, *110*, 13126-13130.
53. Zhao, Y.; Truhlar, D. G. *Theor. Chem. Acc.* **2008**, *120*, 215-241.
54. Weigend, F.; Furche, F.; Ahlrichs, R. *J. Chem. Phys.* **2003**, *119*, 12753-12762.
55. Barone, V.; Cossi, M. *J. Phys. Chem. A* **1998**, *102*, 1995-2001.
56. Okuno, Y. *Chem.-Eur. J.* **1997**, *3*, 212-218.

SYNOPSIS TOC